Observation of Excitons in One-Dimensional Metallic Single-Walled Carbon Nanotubes

Feng Wang,[1] David J. Cho,[1] Brian Kessler,[1] Jack Deslippe,[1] P. James Schuck,[2] Steven G. Louie,[1,2,3] Alex Zettl,[1,3]
Tony F. Heinz,[4] and Y. Ron Shen[1,3]

[1]*Department of Physics, University of California at Berkeley, Berkeley, California 94720, USA*
[2]*Molecular Foundry, Lawrence Berkeley National Laboratory, Berkeley, California 94720, USA*
[3]*Materials Science Division, Lawrence Berkeley National Laboratory, Berkeley, California 94720, USA*
[4]*Departments of Physics and Electrical Engineering, Columbia University, 538 West 120th St., New York, New York 10027, USA*
(Received 12 July 2007; published 28 November 2007)

Excitons are generally believed not to exist in metals because of strong screening by free carriers. Here
we demonstrate that excitonic states can in fact be produced in metallic systems of a one-dimensional
character. Using metallic single-walled carbon nanotubes as a model system, we show both experimen-
tally and theoretically that electron-hole pairs form tightly bound excitons. The exciton binding energy of
50 meV, deduced from optical absorption spectra of *individual* metallic nanotubes, significantly exceeds
that of excitons in most bulk semiconductors and agrees well with *ab initio* theoretical predictions.

Excitons, which are pairs of electrons and holes bound together by their mutual Coulomb interaction, are fundamental to our understanding of optical transitions in semiconductors and insulators [1]. In metals, however, screening of the mutual Coulomb interaction of the electron and hole by free carriers is highly effective. This screening is expected to prevent the formation of excitons, and, correspondingly, no experimental evidence of excitons has been reported in any metallic system. The situation can be very different in one-dimensional materials where the effectiveness of screening is significantly reduced. Indeed, the possibility of forming bound excitons in 1D metals was recently predicted [2,3]. Here we investigate the nature of optical excitations in 1D metals using metallic single-walled carbon nanotubes (SWNTs) as a model system. We found experimentally that the optical transitions in this 1D metallic system are dominated by the excitons and that exciton binding energies can be as large as 50 meV.

Carbon nanotubes can be viewed as rolled up strips of graphene. The structure of a SWNT is consequently defined by the chiral indices (n, m), the projections of the folding vector onto the graphene basis vectors [4,5]. The physical properties of SWNTs depend sensitively on the chiral indices, changing from metallic for mod(n-m, 3) = 0 to semiconducting for mod(n-m, 3) ≠ 0. With diameters on the order of 1 nm and lengths of many microns, SWNTs constitute a model 1D system.

Previous experimental studies of excitons and excitonic binding energies in SWNTs have been performed on semiconducting nanotubes using fluorescence as the probe [6–8]. This technique is not applicable to metallic nanotubes because of their low fluorescence yield. Here we have developed a sensitive form of absorption spectroscopy that allows us to measure directly the optical absorption spectra of *individual* metallic SWNTs. From the line shape of the optical transitions, we can identify the signature of

exciton formation. The experimental spectra also permit a direct determination of the exciton binding energy through identification of the weaker, but clearly observable transitions to the continuum states.

Our spectroscopic measurements were performed on SWNTs suspended across a 25 μm $\times$ 1 mm open slit [Fig. 1(a)] [9]. The SWNTs were grown by chemical-vapor deposition using methane feedstock gas and an alumina supported Fe/Mo catalyst [10]. The nanotubes under study were characterized by high-resolution transmission electron microscopy [Fig. 1(b)]. Under our growth conditions, the suspended nanotubes were tens of microns apart, so that we could easily locate and optically probe a given nanotube.

The absorption spectrum of each individual nanotube was obtained by a direct measurement of the decrease in the transmission that it induced [11]. This method complements photothermal techniques, which have also recently been shown to permit measurement of single nanotube absorption spectra [12]. In our measurement, the optical probe beam, which could be tuned continuously between
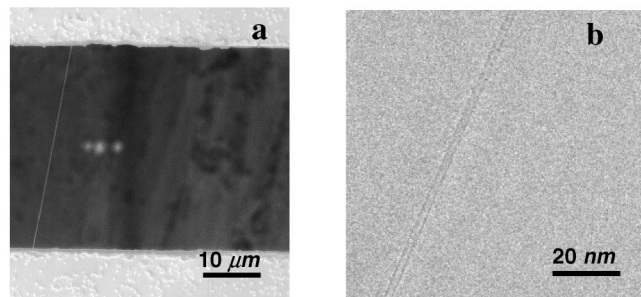

FIG. 1.   (a) Scanning electron micrograph of a carbon nanotube suspended across the slit structure. (b) High-resolution transmission electron micrograph of a single-walled carbon nanotube. It is seen to be free of amorphous carbon.

wavelengths of 510 and 730 nm, was produced by an optical parametric oscillator pumped by an 80-MHz mode-locked Ti:sapphire laser. We use a probe beam with a spectral bandwidth of ~12 meV, power of ≤0.1 mW, and polarization along the nanotube axis. The beam was focused to a spot size of ~2 μm in an optical microscope and illuminated a single nanotube in the focal plane. The transmitted beam was collimated and detected by a photodiode. To measure the slight decrease in transmission ($\sim 10^{-4}$) from the absorption of the nanotube, we modulate the nanotube position periodically at 90 Hz across the laser focal spot and measure the resulting change in the transmitted signal with a lock-in amplifier.

The first step in our study was the identification of the chiral indices of individual suspended nanotubes. This was accomplished using complementary Rayleigh [9,13] and Raman [6,14] spectroscopy, in which we detect, respectively, the elastic and inelastic light scattering into the dark-field. The resonances in Rayleigh cross section yield the energies of the nanotube optical transitions, from which we can deduce the nanotube chiral indices [13]. Figure 2(a) shows the Rayleigh spectrum from an individual nanotube. In this case, the transition energy (1.87 eV) and spectral structure (single peak) indicate that the nanotube is a (21,21) armchair metallic SWNT. The assignment could be double-checked by Raman spectroscopy [Fig. 2(b)] of the radial breathing mode (RBM) on the same nanotube. From the known relation between the RBM frequency and the nanotube diameter [15], we obtain a diameter of 2.9 nm, consistent with the (21,21) assignment. The single, highly-symmetric feature found for the Raman G-mode [Fig. 2(c)] is also characteristic of an armchair metallic nanotube.

After establishing the chiral indices, we measured the absorption spectrum of this (21,21) metallic nanotube [Fig. 3(a)]. The absorption peak at 1.87 eV is consistent with the resonance observed in Rayleigh scattering spectrum and is associated with the second (M_{22}) subband transition of the metallic nanotube.

Does this feature arise from interband transitions of largely noninteracting quasiparticles or from an excitonic transition of strongly correlated electron-hole pairs? For noninteracting quasiparticles, one expects to observe a peak in the absorption spectrum from van Hove singularity in the joint density of states that exists at the band-edge of the 1D nanotube system. Such a picture of noninteracting quasiparticles is compatible with the qualitative features observed in ensemble absorption measurements and follows naturally from the assumption that strong screening in metallic structures should render any residual carrier-carrier interaction unimportant. The availability of accurate absorption spectra of isolated, individual metallic nanotubes now allows a quantitative test of this picture.

We have calculated the expected absorption line shape for the (21,21) nanotube within the tight-binding model. The best fit of this model [black line in Fig. 3(a)], including an empirical broadening and a slight shift of the transition energy, clearly fails to reproduce the experimental spectrum. In particular, in the range close to the peak [dashed box in Fig. 3(a)], the fit is significantly more asymmetrical than the experimental line shape. The symmetry of the observed line shape is a signature of an excitonic transition. The weak additional feature in the high-energy wing of the transition, on the other hand, arises from the residual effect of weak continuum transitions, as we discuss below.

Before we analyze the absorption feature of the armchair metallic nanotube in detail, let us examine the similar feature in a (16,15) semiconducting SWNT [Fig. 3(b)]. The peak in this semiconducting nanotube corresponds to the optical transition from the fourth subband (S_{44}). In semiconducting SWNTs, the optical transitions are known to be dominated by excitons with binding energies of hundreds of meV and to exhibit negligible oscillator strength in the continuum [2,7,8,16–21]. Thus the main peak at 2.01 eV in Fig. 3(b) arises from an excitonic transition. The secondary feature at ~2.21 eV is a phonon sideband, corresponding to simultaneous creation of an exciton and an optical phonon of ~0.2 eV energy [22–
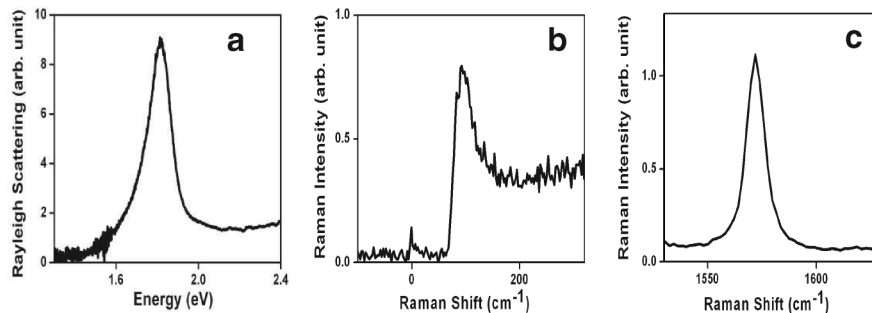

FIG. 2. Spectroscopic analysis of a given, individual SWNT by different optical techniques. (a) The Rayleigh scattering spectrum reveals an optical transition at 1.87 eV. The single peak is characteristic of an armchair metallic nanotube, and the transition energy indicates that it is a (21,21) nanotube. (b) Raman spectrum of the radial breathing mode. The Raman shift of 90 cm^{-1} corresponds to a diameter of 2.9 nm, consistent with the (21,21) assignment. (c) Raman spectrum of the G-mode feature. Its symmetric line shape and single peak also indicate an armchair nanotube.
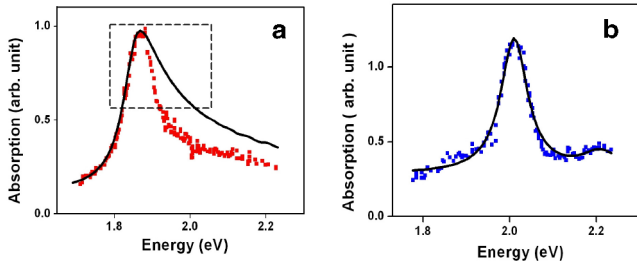
FIG. 3 (color online). Absorption spectra of individual SWNTs. (a) The (21,21) armchair metallic nanotube. The line shape cannot be described by a van Hove singularity within a picture of band-band transitions (black curve). The discrepancy is particularly marked for the spectral range within the dashed box where the experimental line shape is largely symmetric, characteristic of an excitonic transition. (b) The (16,15) semiconducting nanotube. The excitonic effect is much stronger in this semiconducting SWNT and the continuum band-band absorption feature seen in the high-energy tail of (a) is absent. The weak peak located 200 meV above the main resonance is attributed to a phonon side band [22–25]. The absorption line shape is fit by two Lorentzian functions.

25]. The absorption spectrum can be described simply by two Lorenzian lines (black line) with a weak nonresonant background.

Let us now compare the experimental absorption spectra of the metallic and semiconducting nanotubes [Fig. 4(a)]. To facilitate the comparison, we have shifted the energy and rescaled the amplitude of the spectrum for the semiconducting nanotube to match that of the metallic one. The main peaks in the two spectra are seen to be remarkably similar to one another, both arising from excitonic transitions. The difference between the two lies in the much
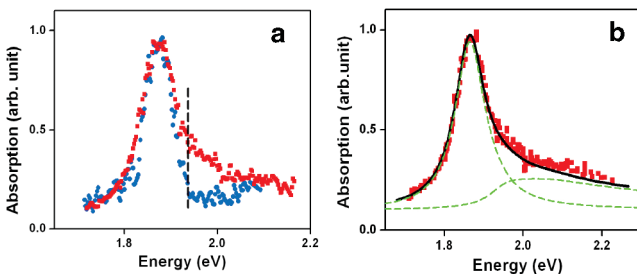

FIG. 4 (color). Detailed analysis of the absorption spectrum of the (21,21) metallic nanotube of Fig. 3(a) (red symbol). (a) Comparison with the experimental absorption feature of the (16,15) semiconducting SWNT of Fig. 3(b) (blue symbol), after a slight shift in energy and adjustment in strength. In the metallic nanotube, absorption from the continuum transitions is apparent in the high-energy wing. From the threshold of the continuum absorption (dashed line), we estimate an exciton binding energy of 50 meV. (b) Comparison of the theory (black solid line) for the optical transition in a metallic nanotube as described in the text. The predicted absorption can be decomposed into the dominant exciton contribution and a continuum contribution (green dashed lines).

stronger high-energy tail in the spectrum of the metallic nanotube. This feature is attributed to the effect of continuum band-to-band transitions for the metallic nanotube. Compared to semiconducting nanotubes, the metallic nanotubes have weaker electron-hole interactions because of screening by the conduction electrons. The result is a smaller exciton binding energy and a corresponding increase of oscillator strength of the continuum transitions [2]. From the rising edge of the continuum contribution [dashed line in Fig. 4(a)], we can estimate the quasiparticle band gap and an exciton binding energy of approximately 50 meV.

For a more quantitative description of the optical transitions and their excitonic features, we have performed *ab initio* electronic structure calculations on armchair metallic SWNTs. In these calculations, we determined the quasiparticle band structure within the GW approximation and then solved the Bethe-Salpeter equation for the exciton states [2]. Results have been obtained for (10,10) nanotubes, since computational limitations do not currently permit direct calculations of large nanotubes. We can, however, use the predicted spectrum of the *first* (M_{11}) subband transition in the (10,10) nanotube as a proxy for the experimentally relevant spectrum of the *second* (M_{22}) subband transition of the (21,21) nanotube. These two transitions involve nearly identical quasiparticle states in the folded Brillouin zone of graphene and their absorption line shapes should be very similar. To test the validity of this procedure, we have applied it to relate the corresponding transitions in the spectra of (10,10) and (5,5) SWNTs for which full *ab initio* calculations are possible. Excellent agreement is found. (See supplementary information [26].) Making use of this procedure to generate theoretical spectra for the (21,21) nanotube, we obtained a direct comparison of theory and experiment for the (21,21) nanotube [Fig. 4(b)]. The theoretical prediction includes an empirical line broadening of 80 meV and a weak constant background absorption. The calculated absolute transition energy is slightly shifted in the comparison. The relative position of the exciton and continuum contributions and their respective strengths are, however, obtained directly from the theory without any modification. The predicted absorption spectrum includes a dominant contribution from the excitonic state [27]. Excellent agreement between the overall predicted line shape and the experimental data is obtained. The small deviation between theory and experiment at ~200 meV above the main transition is attributed to existence of a phonon side band, as was also seen for semiconducting nanotubes. This effect has not been included in the calculation, which treats the lattice as fixed. Comparison of experiment and theory yields an exciton binding energy of 50 meV, consistent with the value obtained above. The calculated exciton radius is 3.1 nm.

The existence of exciton transitions in metals is a distinctive feature of 1D systems. Part of the effect arises, as

discussed in quantum mechanics texts, from the less strin-
gent criteria for bound state in any 1D potential compared
with the behavior in higher dimensions. A second, more
important factor is the drastic reduction of the effectiveness
of free-electron screening in one dimension. To gain an
intuitive picture of this screening, let us consider the
behavior of free electrons within the well-known
Thomas-Fermi model of the momentum dependent, static
dielectric function $\varepsilon(q)$[1]. For 3D metals, the Thomas-
Fermi approach predicts $\varepsilon(q) = 1 + k_0^2/q^2$, where k_0 is a
constant of the order of 1 Å^{-1} and q is the wave vector of
the external potential. In real space this yields a Yukawa
potential for a point charge, with a potential decaying
exponentially at distance larger than ~ 1 Å. For 1D metals
(supplementary material), screening is described by
$\varepsilon(q) = 1 + 2e^2 \mathrm{DOS} I_0(qd/2)K_0(qd/2)$, where DOS de-
notes the 1D density of states at the Fermi level, e is the
electron charge, d is the nanotube diameter and $I_0(x)$ and
$K_0(x)$ are modified Bessel functions. One can evaluate the
relevant parameters using the tight-binding model [4]. For
small wave vectors q, the free-electron screening in 1D
diverges only logarithmically, in contrast to the power-law
dependence in the 3D case. Thus in one dimension, the
Coulomb potential of a charge remains largely unscreened
over a considerable range in real space. If we consider an
electron-hole separation characteristic of the calculated
exciton radius of $R_{\mathrm{ex}} \approx 3$ nm, the important Fourier com-
ponents in the dielectric screening function will be those
with wave vectors in the range of $1/R_{\mathrm{ex}}$. The dielectric
function for conduction electron screening is then found to
be ~ 7. It is this relatively ineffective screening, which is
orders of magnitude weaker than that found in a bulk
metal, that allows strong excitonic interactions in 1D
metals.

The excitonic character of the optical transitions in
metallic nanotubes demonstrates the important role of
Coulomb interactions and the corresponding many-body
interactions in systems of reduced dimension. Since the
underlying physics arises from considerations of dimen-
sionality rather than any specific properties of nanotubes,
excitonic interactions are likely to be significant in other
strongly 1D metallic systems. This conclusion highlights
the fact that well-established concepts for bulk materials,
such as nearly perfect screening in metals, can fail in
systems of lower dimensionality.

[1] N. W. Ashcroft and N. D. Mermin, *Solid State Physics*
(Brooks-Cole, Belmont, 1976).
[2] C. D. Spataru *et al.*, Phys. Rev. Lett. **92**, 077402 (2004).
[3] J. Deslippe *et al.*, Nano Lett. **7**, 1626 (2007).
[4] R. Saito, G. Dresselhaus, and M. S. Dresselhaus, *Physical
Properties of Carbon Nanotubes* (Imperial College,
London, 1998).
[5] S. Reich, C. Thomsen, and J. Maultzsch, *Carbon Nano-
tubes. Basic Concepts and Physical Properties* (Wiley-
VCH, Weinheim, 2004).
[6] S. M. Bachilo *et al.*, Science **298**, 2361 (2002).
[7] F. Wang *et al.*, Science **308**, 838 (2005).
[8] J. Maultzsch *et al.*, Phys. Rev. B **72**, 241402 (2005).
[9] M. Y. Sfeir *et al.*, Science **306**, 1540 (2004).
[10] J. Kong *et al.*, Nature (London) **395**, 878 (1998).
[11] Scattering loss is negligible compared with absorption for
small objects like SWNTs.
[12] S. Berciaud *et al.*, Nano Lett. **7**, 1203 (2007).
[13] M. Y. Sfeir *et al.*, Science **312**, 554 (2006).
[14] M. S. Dresselhaus *et al.*, Acc. Chem. Res. **35**, 1070 (2002).
[15] M. J. O'Connell *et al.*, Science **297**, 593 (2002).
[16] V. Perebeinos, J. Tersoff, and P. Avouris, Phys. Rev. Lett.
92, 257402 (2004).
[17] T. Ando, J. Phys. Soc. Jpn. **66**, 1066 (1997).
[18] T. G. Pedersen, Phys. Rev. B **67**, 073401 (2003).
[19] T. Ogawa and T. Takagahara, Phys. Rev. B **44**, 8138
(1991).
[20] H. B. Zhao and S. Mazumdar, Phys. Rev. Lett. **93**, 157402
(2004).
[21] C. L. Kane and E. J. Mele, Phys. Rev. Lett. **93**, 197402
(2004).
[22] X. H. Qiu *et al.*, Nano Lett. **5**, 749 (2005).
[23] H. Htoon *et al.*, Phys. Rev. Lett. **94**, 127403 (2005).
[24] S. G. Chou *et al.*, Phys. Rev. Lett. **94**, 127402 (2005).
[25] V. Perebeinos, J. Tersoff, and P. Avouris, Phys. Rev. Lett.
94, 027402 (2005).
[26] See EPAPS Document No. E-PRLTAO-99-036747 for
supplementary information. For more information on
EPAPS, see http://www.aip.org/pubservs/epaps.html.
[27] The same Coulomb interactions that give rise to bound
excitonic states suppress and spectral modify the sharply-
peaked feature expected from van Hove singularity in the
joint density of quasiparticle states (Ref. [19]).